Design of periodic metal-insulator-metal waveguide back structures for the enhancement of light absorption in thin-film solar cells*

Zheng Gai-Ge(郑改革), Jiang Jian-Li(蒋剑莉), Xian Feng-Lin(咸冯林), Qiang Hai-Xia(强海霞), Wu Hong(武 虹), and Li Xiang-Yin(李相银)†

School of Science, Nanjing University of Science and Technology, Nanjing 210094, *China*

(Received 14 December 2010; revised manuscript received 24 January 2011)

To increase the absorption in a thin layer of absorbing material (amorphous silicon, a-Si), a light trapping design is presented. The designed structure incorporates periodic metal-insulator-metal waveguides to enhance the optical path length of light within the solar cells. The new design can result in broadband optical absorption enhancement not only for transverse magnetic (TM)-polarized light, but also for transverse electric (TE)-polarized light. No plasmonic modes can be excited in TE-polarization, but because of the coupling into the a-Si planar waveguide guiding modes and the diffraction of light by the bottom periodic structures into higher diffraction orders, the total absorption in the active region is also increased. The results from rigorous coupled wave analysis show that the overall optical absorption in the active layer can be greatly enhanced by up to 40%. The designed structures presented in this paper can be integrated with back contact technology to potentially produce high-efficiency thin-film solar cell devices.

Keywords: thin-film solar cells, metal-insulator-metal waveguide, enhanced optical absorption, rigorous coupled wave analysis

PACS: 42.15.Eq, 42.79.–e, 42.82.Bq **DOI:** 10.1088/1674-1056/20/9/094201

1. Introduction

Solar cell technology is considered to be one of the main methods to satisfy the critical need for renewable, non-fossil fuel sources of energy. The active material used in thin-film solar cells (TFSC) is usually silicon (polysilicon, p-Si or amorphous silicon, a-Si), which is considered to be one of the best candidates for the large-scale photovoltaic conversion of sunlight.[1−5] However, due to the short carrier diffusion length in silicon, to achieve nearly complete absorption, the absorbing layer's thickness should be at least a few micrometers (μm). This in turn requires the use of pure materials with a long minor carrier diffusion length, which increases costs and energy payback time. Thus, a careful optical design of the device structure is crucial for optimizing light trapping and absorption in TFSCs.

Light trapping in silicon solar cells falls mainly into two categories: the first is the reduction of front surface reflection and the second involves increasing the optical path length of light within the cell.[2] The concept of reducing surface reflectivity by introducing intermediate transparent layers such as silicon dioxide (SiO_2), silicon nitride (Si_3N_4) and some transparent conductive oxides has been known since the early 1800s.[6] To increase the optical path length of light, numerous strategies and designs inspired from nanophotonics have emerged, ranging from planar reflective surfaces to arrays of ordered nanostructures integrated on the back surface. Among them, periodic nanometallic structures have attracted a rapidly growing interest because they offer new approaches to the altering and tailoring of the basic optical properties of materials.[7−9] Through proper design of the structural parameters, one can widely tune the optical absorption due to the surface plasmon (SP),[8,9] which is an optically generated wave that propagates along the interface between a metal and the dielectric material. Among a wide field of applications, the SP can be used in the photovoltaic domain, especially in spectral bands where materials absorb weakly, in order to improve photonic absorption and correspondingly improve solar cell efficiency.

*Project supported by the Postgraduate Innovation Foundation of Jiangsu Province, China (Grant No. CX09B_090Z) and the Key Postgraduate Plan of Nanjing University of Science and Technology, China.

†Corresponding author. E-mail: jsnanophotonics@yahoo.com

© 2011 Chinese Physical Society and IOP Publishing Ltd

In this paper, we propose the placement of periodic metal-insulator-metal (MIM) waveguides at the bottom of the optically active layer, which is shown in Fig. 1. By investigating the use of MIM waveguides on the backside of solar cell, this design will not only free up those photons blocked by surface nanostructures in designs with metallic structures placed on the front surface of solar cells, but also achieve broadband and polarization-insensitive absorption enhancement. The design was carefully examined by the rigorous coupled wave analysis (RCWA) method and a remarkable 40% light absorption improvement was anticipated for the design in comparison with bare a-Si TFSCs. The processes for the fabrication of these structures can be divided into several common steps comprised primarily of plasma-enhanced chemical vapour deposition, electron beam lithography and inductively coupled plasma etching.

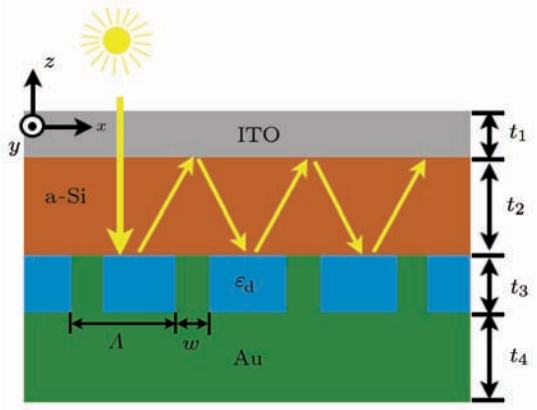


Fig. 1. (colour online) A cross-sectional view of the proposed solar cell structure.

2. Solar cell system design and rigorous calculation

Due to the sub wavelength feature sizes associated with the nanostructured waveguides, a rigorous electromagnetic simulation tool is required and hence we opt to use the RCWA method,[10−13] which is also known as the Fourier modal method. The RCWA method is also able to incorporate any lossy (even in metallic materials) and dispersive (frequency dependent) materials. A schematic picture of a simple case using the RCWA method is shown in Fig. 2. The periodic structure can be decomposed into several layers with the constraint that each layer has the same periodicity. The fields inside each layer are expanded in terms of in-plane spatial harmonics, whose amplitudes are allowed to vary in the out-of-plane direction. The fields in the superstrate and substrate regions are described by the Rayleigh expansion. The wave vectors of these diffracted orders outside of the periodic structure are phase-matched to the in-plane spatial harmonics inside the structure.[11] The electromagnetic problem consists of solving the variations of the amplitudes of the spatial harmonics along the out-of-plane direction. The fields are then boundary matched to calculate the amplitudes of the Rayleigh orders in the superstrate and substrate. This way of solving the Maxwell's equations allows the calculation of the reflectance R, the transmittance T and thus of the absorption $A = 1 - R - T$ of a plane wave incident on our structures, as well as the plot of the electromagnetic field distribution in the structure.[12] In addition, due to the ability to calculate the optical response of a metallic material and the manipulation in Fourier domain, the RCWA method is much more efficient than volumetric numerical electromagnetic techniques such as the finite element method and the finite-difference time-domain method. The accuracy of RCWA depends on the number of diffraction modes retained in the structure.

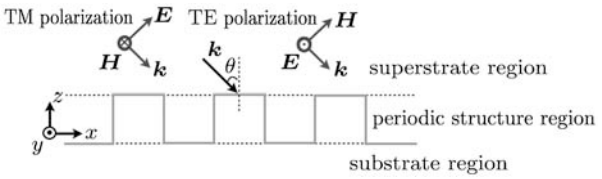


Fig. 2. Schematic picture of a simple case using the RCWA method. The light is launched from the superstrate region. In the algorithm of the RCWA method, all of the periodic structures will be split into many simple periodic forms.

We made several modifications to our RCWA code to allow for rigorous calculation of our hybrid structure. Mirror symmetries were exploited for faster convergence with fewer diffraction orders. The eigenvalue problem in each layer of the two-dimensional (2D) periodic structure was set up in terms of two second-order differential equations rather than four first-order equations, which improved the computational efficiency by a factor of eight. A two-dimensional generalization of the enhanced transmittance matrix method was also used to enforce boundary conditions at the interface of two layers.[13] Greater accuracy can be obtained without increasing computational requirements.

The basic idea of using periodic elements at the bottom of a solar cell is to change the direction of light

propagation inside the solar cell. Metallic waveguides can be efficient at exciting SPs at their interfaces and therefore confine electromagnetic waves in the near field and couple light into absorbing materials to enhance absorption.[8,9] By optimizing the period and height of the MIM structure, we can achieve a high diffraction efficiency in a certain spectral range. The principal ideas are sketched in Figs. 1 and 2. From the absorption within the a-Si layer, we will calculate the optical absorption of an air mass 1.5 solar spectrum within a spectral range from 400 nm to 1000 nm. The geometrical parameters of the structure to be optimized are scanned and RCWA simulation is performed for each set of parameters. Experimentally measured data for the complex dielectric constants of materials are used in the calculation.[14]

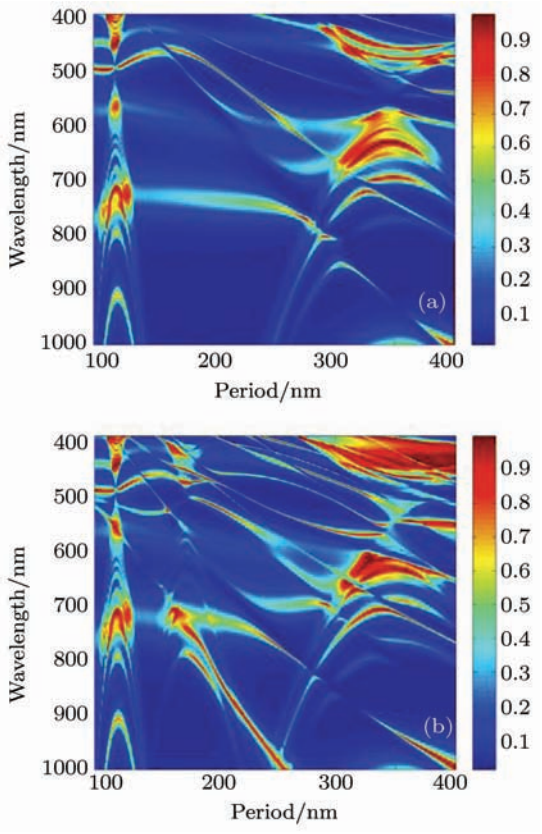


Fig. 3. (colour online) The absorption with varying period of MIM waveguides: (a) incident angle is 0°; (b) incident angle is 30°. By changing the period of the MIM waveguide, an RCWA simulation was performed for each wavelength.

3. Numerical analyses and discussion

To simplify our discussion, the top layer's thickness (indium tin oxide, ITO) is fixed at $t_1 = 20$ nm and the waveguide width w is fixed at 50 nm. The thickness of the active region and substrate, and the height of the MIM waveguide are $t_2 = 200$ nm, $t_4 = 100$ nm and $t_3 = 50$ nm, respectively. The insulator can be chosen with suitable dielectric materials, which can provide an additional ability to fine-tune the dielectric environment of the nanowaveguide. Here, we choose all of the insulator material as ITO. The simulation results, obtained from mapping absorption with different structural parameters and incident conditions, are shown in Fig. 3. Figures 3(a) and 3(b) correspond to 0° and 30° incident angles, respectively. It is very interesting that in the long wavelength range, Fig. 3 shows a few areas in which large light absorption occurs. When the incident angle is 30°, the large light absorption area will be enlarged in comparison with the 0° case. For an illustration of the results, the transverse magnetic (TM) wavelength-dependent absorption spectrum is shown in Fig. 4, where we select the MIM waveguide period at 350 nm and incident angle at 30°. In this paper, a TM-polarized electromagnetic wave is defined such that the magnetic field is parallel to the integrated structure's surface and the electric field oscillates in the incident plane; while, in contrast, the transverse electric (TE)-polarized wave has no electric field component normal to the surface (see Fig. 2).

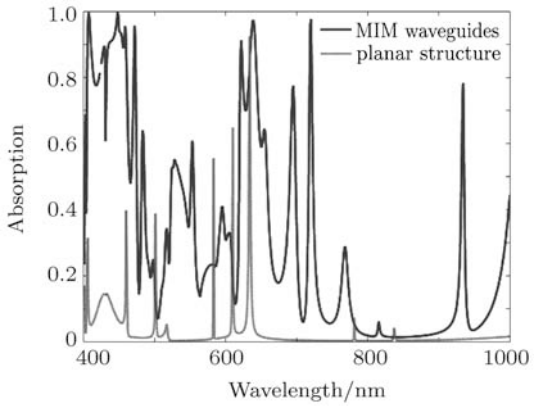


Fig. 4. Absorption spectra at the a-Si thickness of 200 nm, under TM illumination with the grating periods of 350 nm and incident angle of 30°.

Photons with wavelengths below 0.65 μm can be absorbed effectively in a thin a-Si layer. However, when $\lambda > 0.65$ μm, the absorption length exceeds 1 μm and in the near-infrared (NIR) below the bandgap wavelength (0.7–0.775 μm), the absorption length exceeds 5 μm. It is very difficult to harvest these NIR photons. In our design, even the thickness of the a-Si layer is only 200 nm, which can improve the

absorption in NIR remarkably. Compared with the case without the MIM waveguides (planar structure), significant differences will be required to enhance absorption occurring at a certain long wavelength and to enhance broadband absorption. In Fig. 4, the long-wavelength absorption enhancement is obvious after the addition of the MIM waveguides. Most of the enhanced absorption occurs in the longer wavelength region, where photons have long absorption lengths. The periodic metallic waveguides generate plasmonic modes at these wavelengths, effectively helping the optical absorption within the TFSC.[3,15] Surface plasmon polariton (SPP) modes can be excited around the waveguide structures, which have the characteristic of being excited only by TM polarization. The SPP wave vector is given by[7]

$$\boldsymbol{k}_{\rm sp} = \boldsymbol{k}_0 \left(\frac{\varepsilon_{\rm ITO}\varepsilon_{\rm Au}}{\varepsilon_{\rm ITO} + \varepsilon_{\rm Au}} \right)^{1/2}, \tag{1}$$

where $\boldsymbol{k}_{\rm sp}$ is parallel to the interface and $\boldsymbol{k}_0$ is the wave vector at vacuum. The mismatch in wave vector between the in-plane momentums can be achieved by patterning periodic structures with a period Λ. For the one-dimensional and normal incident case, phase matching will happen when

$$\frac{2\pi}{\Lambda} = \boldsymbol{k}_0 \left(\frac{\varepsilon_{\rm ITO}\varepsilon_{\rm Au}}{\varepsilon_{\rm ITO} + \varepsilon_{\rm Au}} \right)^{1/2}. \tag{2}$$

For rectangular shapes, strong confinement of light and the coupling of light into the absorbing layer mostly occur at the upper surface of a waveguide.[15,16] Compared with the reference, the SPP back structures can obviously increase the total absorption in the wavelength range from 600 nm to 1000 nm, which is an optimized spectral range to absorb the solar energy.

If the incident light is TE polarized, no plasmonic mode can be excited. MIM periodic waveguides can be seen as 1D photonic crystals that provide diffraction of photons and increase the photon path length within the absorber layer. The solar cell with MIM structures can achieve absorption that is considerably larger than that without the MIM waveguides (Fig. 5). The MIM waveguides generate modes of diffraction at wavelengths which effectively increase the path length.[17] The large enhancement around 800 nm can be attributed to the excitation of a-Si planar waveguide guiding modes.[3] The coupling into this planar waveguide mode is affected by a-Si layer thickness, MIM waveguide period, and polarization, but much less affected by the MIM waveguide's height. Compared with the common textured back reflector, the MIM waveguide hybrid structure can achieve much greater enhancement at resonance wavelengths where even the incident light is not TM polarized.

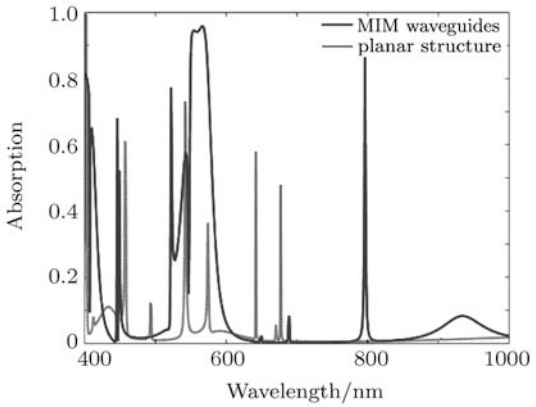


Fig. 5. Absorption spectra at the a-Si thickness of 200 nm, under TE illumination with the grating periods of 350 nm and an incident angle of 60°, the other parameters are the same as those in Fig. 3.

When light is incident on this integrated solar cell, the scattering of light waves is affected by the following processes. First, the incident light undergoes typical diffraction on the nanostructured hybrid structure. The incident wavelengths that can be diffracted at angles nearly parallel to the interface, where the waveguides modes are generated, will be strongly absorbed in the solar cell. The condition for this mechanism to occur is that the round-trip phase difference between the light waves from the bottom and top of the absorbing layer is an integral multiple of 2π. However, exploiting the periodic structure based on the excitation of guided modes in the a-Si layer is most effective in the spectral range, where silicon shows low absorption (red and infrared part of the optical spectrum).[18]

Second, when a resonant condition is met, the incident light excites SPPs, which propagates along the surface of the nanostructure.[19,20] The high electric field and concentration of light at resonant frequencies generate high absorption of the incident wavelength. Surface features induce changes to the dispersion relations of SPPs owing to the interaction between the SPPs and the surface features. As a result, SPPs scatter into other SPPs propagating in other directions, or decay by emitting photons.

The third mechanism can be exploited based on the diffraction of light by the bottom periodic structures into higher diffraction orders. If the period of the

waveguide is sufficiently large to allow diffraction orders to propagate inside the absorbing layer, the path of the photons is prolonged in comparison with the thin film without a periodic waveguide and the probability for a photon to be absorbed is larger. Constructive interference of the different diffracted orders plays an important role in maximizing the absorption in the absorber layer.

One can see that the strong resonances appearing above 630 nm in the case of the periodic MIM waveguides are strongly reduced for TE polarization (Fig. 5) and vanish almost completely for TM polarization in the case of the planar structure (Fig. 4). Due to the direct contact between a-Si and metal, resonances cause a high electric field at the metal surface and lead to strong absorption, as the imaginary part of the dielectric function of gold is much higher than that of a-Si in this wavelength region.[18]

In TE polarization case, no plasmonic modes can be excited, but when the condition for the excitation of guided modes in the silicon layer is satisfied, the absorption will still be enhanced. The location of peaks in the absorption spectrum can be attributed to the coupling of incident light into guided modes in the solar cell layer. A series of absorption peaks appear in Fig. 5 and each peak corresponds to a mode with good impedance matching with regard to the incident light. There is a large enhancement of absorption between 540 nm and 600 nm, which is the result of the excitation of guided modes and the interference with the zero and the first diffracted order of two neighbouring unit cells. The observed high absorption peaks clearly illustrate that the introduced periodic MIM waveguides play an important role in the control of incident light coupling and in the photon interaction with the absorbing medium. Combining the different effects, we find that the periodic metallic structures on the back surface clearly increase the absorption efficiency of the hybrid solar cell both at short and at long wavelengths.

The calculated total absorption in the active layer is weighted by the air mass 1.5 solar spectrum and integrated from 400 nm ($\lambda_{\min}$) to 1000 nm ($\lambda_{\max}$) to obtain the average absorption $\langle A\rangle$ as [17]

$$\langle A\rangle = \int_{\lambda_{\min}}^{\lambda_{\max}} A(\lambda)\frac{\mathrm{d}I}{\mathrm{d}\lambda}\mathrm{d}\lambda, \tag{3}$$

where $\mathrm{d}I/\mathrm{d}\lambda$ is the incident solar radiation intensity per unit wavelength, $A(\lambda)$ is the total absorptivity and can be defined as

$$A(\lambda) = \frac{A_{\mathrm{TM}}(\lambda) + A_{\mathrm{TE}}(\lambda)}{2}. \tag{4}$$

Here,

$$A_{\mathrm{TM}}(\lambda) = \frac{\int_{\lambda_{\min}}^{\lambda_{\max}} a_{\mathrm{TM}}(\lambda)S(\lambda)\mathrm{d}\lambda}{\int_{\lambda_{\min}}^{\lambda_{\max}} S(\lambda)\mathrm{d}\lambda},$$
$$A_{\mathrm{TE}}(\lambda) = \frac{\int_{\lambda_{\min}}^{\lambda_{\max}} a_{\mathrm{TE}}(\lambda)S(\lambda)\mathrm{d}\lambda}{\int_{\lambda_{\min}}^{\lambda_{\max}} S(\lambda)\mathrm{d}\lambda}, \tag{5}$$

where $a_{\mathrm{TM}}(\lambda)(a_{\mathrm{TE}}(\lambda))$ is the optical absorption spectrum in active layers for TM- (TE-) polarized light and $S(\lambda)$ is the solar irradiance spectrum.

We show the total average absorption $\langle A\rangle$ as a function of MIM waveguide periodicity with a constant depth of diffraction grating for normally incident light in Fig. 6, and two distinct absorption peaks can be seen. By varying the a-Si layer thickness, one can see Fabry–Perot (FP) cavity resonance, which is also helpful for the enhancement of light absorption in a TFSC. After adding the periodic waveguides, the effective thickness of the cavity will actually be changed.[21] Therefore, adjusting the periodic structure is a practical means to tune the FP resonance to better fit the solar spectrum without the need to change the a-Si layer thickness.[18,21] The absorption peaks in Fig. 6 are the results of FP resonance in the cavity. We also find that the coupling of the zero and the first diffraction orders occurs when the periodicity is around 350 nm, which is the reason why the value of the second peak is larger than the first one. In order for the different orders to interfere, the propagating angle of the mode is an important parameter. These angles are governed by the grating equation

$$(\sin\theta_m + \sin\theta_0)\cdot\Lambda\cdot n = m\cdot\lambda,$$
$$m = (\ldots, -1, 0, 1, \ldots), \tag{6}$$

where Λ is the period of the back-surface periodic structure, n denotes the refractive index of the propagating media after diffraction, λ is the wavelength, m specifies the diffraction order, and θ and θ_m correspond to incident angle and diffraction angle, respectively.

The average absorption is optimized for period around 350 nm. Compared with bare a-Si TFSCs, a remarkable 40% light absorption improvement is anticipated from our design. Finally, a generally valid remark on the analysed phenomena needs to be

made. All three mechanisms will affect the encountered absorption enhancement in the analysed structures. However, due to interdependencies, they cannot always be differentiated in their impact. In complex physical systems there are always trade-offs when choosing a proper design strategy.

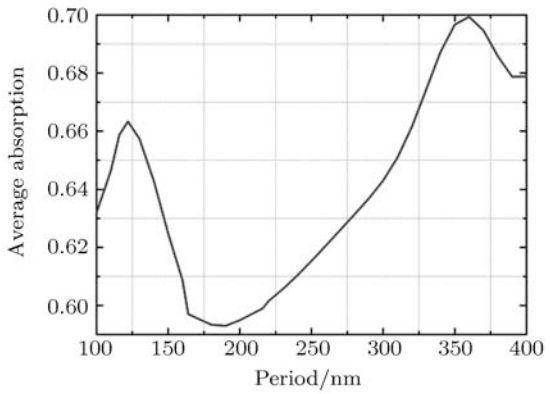


Fig. 6. The variation in average absorption with the period of the MIM waveguides, holding other parameters constant near the optimum values.

4. Conclusion

In summary, the ability to realize large, broadband and polarization-insensitive absorption enhancement will be crucial for practical TFSCs. It is believed that plasmon-assisted schemes are promising for light trapping, which is potentially useful for TFSCs. However, plasmonic modes can only be excited by TM polarized light. If one can design plasmonic structures which can also help the enhancement of optical absorption in the TE-polarization case, the total absorption will be enhanced greatly. We have designed one novel TFSC structure by using the RCWA method. The advantage of this approach is that any number of layers of different widths can be easily simulated since a real-space grid is not necessary. The calculated results show that absorption enhancement not only happens in the TM-polarization case, but also can be witnessed in TE polarization, which is directly attributed to the existence of periodic structures on the back surface. The MIM waveguide hybrid structure presented in this paper is an effective approach to light trapping in TFSC devices.

Acknowledgments

We thank Dr. L X Shi, L H Xu and L Y Jiang for their useful discussions.

References

[1] Daif O E, Drouard E, Gomard G, Kaminski A, Fave A, Lemiti M, Ahn S, Kim S, Cabarrocas P R, Jeon H and Seassal C 2010 *Opt. Express* **18** A293

[2] Mutitu J G, Shi S Y, Chen C H, Creazzo T, Barnett A, Honsberg C and Prather D W 2008 *Opt. Express* **16** 15238

[3] Pala R A, White J, Barnard E, Liu J and Brongersma M L 2009 *Adv. Mater.* **21** 3504

[4] Lee Y C, Huang C F, Chang J Y and Wu M L 2008 *Opt. Express* **16** 7969

[5] Chutinan A and John S 2008 *Phys. Rev.* A **78** 023825

[6] Catchpole K R, McCann M J, Weber K J and Blakers A W 2001 *Sol. Energy Mater. Sol. Cells* **68** 173

[7] Barnes W L, Dereux A and Ebbesen T W 2003 *Nature* **424** 824

[8] Cole J and Halas N J 2006 *Appl. Phys. Lett.* **89** 153120

[9] Akimov Y A, Koh W S, Sian S Y and Ren S 2010 *Appl. Phys. Lett.* **96** 073111

[10] Hooper I R and Sambles J R 2004 *Phys. Rev.* B **70** 045421

[11] Moharam M G, Pommet D A, Grann E B and Gaylord T K 1995 *J. Opt. Soc. Am.* A **12** 1077

[12] Marius P, Marc R, Martin H and Benedikt B 2010 *Proc. SPIE* **7725** 772514

[13] Mallick S B, Agrawal M and Peumans P 2010 *Proc. SPIE* **7725** 772503

[14] Palik E D 1985 *Handbook of Optical Constants of Solids* (Orlando: Academic Press) p. 236

[15] Bai W L, Gan Q Q, Bartoli F, Zhang J, Cai L K, Huang Y D and Song G F 2009 *Opt. Lett.* **34** 3725

[16] Zhou X, Li H J, Xie S X, Fu S L, Xu H Q and Wu J J 2010 *Chin. Phys.* B **19** 127806

[17] Zhou D Y and Biswas R 2008 *J. Appl. Phys.* **103** 093102

[18] Matthias K, Stephan F, Christian H, Carsten R, Falk L and Thomas P 2008 *Phys. Stat. Sol.* (a) **205** 2777

[19] Chen H B, Chen X S, Li H J, Lu W, Wang L L, Wang S W, Hui X Zeng Y, Zhang J B and Zhou R L 2008 *Acta Phys. Sin.* **57** 3506 (in Chinese)

[20] Bai W L, Guo B S, Cai L K, Gan Q Q and Song G F 2009 *Acta Phys. Sin.* **58** 8021 (in Chinese)

[21] Li L, Lu W X and Lu Y L 2010 *Mater. Sci. Forum* **636** 860